Surface Chemistry of Monochlorinated and Dichlorinated Benzenes on Si(100)2×1: Comparison Study of Chlorine Content and Isomeric Effects

X. J. Zhou and K. T. Leung*

Department of Chemistry, University of Waterloo, Waterloo, Ontario N2L 3G1, Canada

Received: January 15, 2006; In Final Form: March 20, 2006

Using X-ray photoelectron spectroscopy (XPS) and temperature-programmed desorption (TPD), the room temperature (RT) adsorption and thermal evolution of monochlorobenzene (MCB) and 1,3-dichlorobenzene (1,3-DCB) on Si(100)2×1 have been investigated and compared with that of 1,2-dichlorobenzene (1,2-DCB) reported previously. Like 1,2-DCB, the C 1s features observed at 284.6 (C_1) and 286.0 eV (C_2) for both MCB and 1,3-DCB could be attributed to the C−H and C−Cl bonds, respectively. The C_1/C_2 intensity ratios for MCB (5.0) and 1,3-DCB (2.0) are found to follow the stoichiometric ratios of the C−H to C−Cl bonds for MCB and 1,3-DCB, respectively, indicating that both MCB and 1,3-DCB adsorb on Si(100)2×1 molecularly with negligible C−Cl dissociation at RT, in marked contrast to the partial C−Cl dissociation found for 1,2-DCB. Unlike 1,2-DCB with two discernible Cl 2s features at 270.3 and 271.2 eV, a single Cl 2s feature at 271.2 eV is observed for MCB and 1,3-DCB, in accord with the single local chemical environment for Cl. The TPD results show that MCB undergoes molecular desorption exclusively, similar to that found for benzene. Both molecular desorption and recombinative HCl desorption are found for 1,3-DCB, similar to that for 1,2-DCB. Despite the different Cl contents and relative Cl locations on the benzene ring, both MCB and 1,3-DCB exhibit RT adsorption behavior remarkably similar to that of benzene. To explain the C−Cl dissociation observed for 1,2-DCB, we propose a possible transition state involving the Cl atoms located at more physically compatible positions with the surface Si dimers in order to facilitate the conversion of 1,2-DCB (preferentially over 1,3-DCB) to dissociated products at RT. However, the thermal evolution of 1,3-DCB is closer to that of 1,2-DCB than that of MCB and benzene. The breakage of C−Cl bonds is found to occur at a relatively low temperature of 425 K, which suggests a relatively low activation barrier for the dechlorination of 1,3-DCB adspecies. Calculated energetics for 1,4-DCB on Si(100)2×1 shows that double dechlorination is not as favorable a process as those for 1,2-DCB and 1,3-DCB.

1. Introduction

Silicon surfaces are important substrates that have been extensively used for fabricating microelectronic and nanoscale devices in the semiconductor industry.[1−5] As the demand for electronics miniaturization continues, direct attachment of functionalized organic molecules to the silicon surfaces appears promising for developing devices approaching the molecular scale. In particular, Si(100)2×1 and Si(111)7×7 are two of the most studied semiconductor surfaces because of their unique surface structures with directional and chemically active dangling bonds. Organic molecules with π or lone-pair electrons are found to react readily with these surfaces. The wide variety of the resulting adstructures[6−21] could potentially be used as the interface for building molecular electronic devices.[2] The strong chemical bonds in these adstructures could, in effect, serve as conduits for electron transfer between the substrate and any linkage molecules that could interact with and/or attach to the adstructures. Depending on the sizes and electronic properties of the linkage molecules, molecular chains or highly ordered two-dimensional templates could also be assembled on these interfaces.[22,23] Judicious choice of organic admolecules could provide appropriate functional groups for reacting with selective surface sites and for linkage with other molecules. Understanding the reaction mechanisms of the selected admolecules on the silicon surface is therefore important not only to the development of the organo-silicon interface but also ultimately to the optimization of the device performance.

As the most popular aromatic molecule, benzene has been extensively studied as a benchmark admolecule on silicon surfaces, especially Si(100)2×1, by a variety of experimental techniques and computational methods.[6,8,12,24−26] Despite the voluminous amount of work, the nature of exactly how benzene attaches to the silicon surface remains under debate. At issue are some of the key questions, including the number of benzene adstructures on Si(100)2×1 and the relative stabilities of these adstructures.[12,25] Furthermore, substituted derivatives of benzene that replace H atoms on the ring with chemically active functional groups (including amine[9] and the halogen atom[27−34]) have attracted a lot of recent attention. Some of these studies examine the reaction mechanisms and the possibilities of generating an organo-silicon interface by manipulating the frontier orbitals and the energy gaps of the adstructures. Substituting H atoms with more electron-donating methyl groups in methyl-substituted benzenes (including toluene and *m*-, *o*-, and *p*-xylene) on Si(100)2×1 has also been investigated.[10,15,19,35] The observation of a Si−H stretching mode on Si(100) at room temperature (RT) reported in a Fourier transform infrared (FTIR) spectroscopic study has provided evidence for H abstraction from the methyl group.[35] Our temperature-programmed desorption (TPD) studies have further shown that the stronger

* Corresponding author. E-mail: tong@uwaterloo.ca.

10.1021/jp060286f CCC: $33.50
Published on Web 04/27/2006

recombinative H_2 desorption feature is due to enhanced surface reactions resulting from H abstraction.[15,19] Recently, we presented TPD and X-ray photoelectron spectroscopy (XPS) data on three 1,2-dihalogenated benzenes, namely, 1,2-difluorobenzene (1,2-DFB), 1,2-dichlorobenzene (1,2-DCB), and 1,2-dibromobenzene (1,2-DBB), on Si(100)2×1.[27] Both kinetics and thermodynamics were found to play important roles in governing the emergence and indeed the evolution of specific adstructures. A competition between molecular adsorption and dissociative adsorption was observed for the three 1,2-dihalogenated benzene adsorbates. In particular, 1,2-DFB was found to molecularly adsorb onto the 2×1 surface exclusively, in contrast to 1,2-DBB, which predominantly adsorbs dissociatively. In the case of 1,2-DCB, both molecular and dissociative adsorption were observed with 25% of the C−Cl bonds found to undergo dissociation. Furthermore, a scanning tunneling microscopy (STM) study on halogenated benzenes on Si(100)2×1 reported a novel adspecies that bridges two dimer rows with and without breaking the C−Cl bonds.[33] Further investigations into the adsorption of chlorinated benzenes with different chlorine contents and isomeric structures are therefore of interest not only to gain fundamental insight into their intricate surface chemistries, but also to develop practical protocols for manipulating these adstructures as building blocks for molecular electronics applications. In the present work, we present TPD and XPS data for the RT adsorption and thermal evolution of monochlorobenzene (MCB) and 1,3-dichlorobenzene (1,3-DCB) on Si(100)2×1. In an effort to gain a better understanding of our observations, we also perform ab initio computational studies of possible adsorption models for MCB, 1,3-DCB, and 1,4-dichlorobenzene (1,4-DCB) on a double-dimer $Si_{15}H_{16}$ cluster surface. It should be noted that the vapor pressure of 1,4-DCB, present as a solid, at RT is too low for our present experimental setup. These experimental and computational results are compared with those obtained for 1,2-DCB reported in our recent work.[27]

2. Experimental and Computational Details

All the experiments were performed in a home-built dual-chamber ultrahigh vacuum system with a base pressure better than 1×10^{-10} Torr. Details of our experimental setup and procedures have been described elsewhere.[10] Briefly, the sample preparation chamber was equipped with an ion-sputtering gun for sample cleaning, and four-grid retarding-field optics for both reverse-view low-energy electron diffraction (LEED) and Auger electron spectroscopy. The analysis chamber was used to conduct TPD experiments by using a differentially pumped 1−300 amu quadrupole mass spectrometer and XPS studies by using an electron spectrometer (consisting of a hemispherical analyzer of 100 mm mean radius and a triple-channeltron detector) along with a twin-anode X-ray source that supplied unmonochromatic Al Kα radiation (with a photon energy 1486.6 eV).[17] For the present TPD experiments, a home-built programmable proportional-integral-differential temperature controller was used to provide linear temperature ramping at an adjustable heating rate, typically set at 2 K/s.[10] The temperature was calibrated by the desorption of dihydride at 680 K and that of monohydride at 800 K on Si(100)2×1.[36,37] XPS spectra were collected with an acceptance angle of ±4° at normal emission from the silicon sample and with a constant pass energy of 50 eV, giving an effective energy resolution of 1.4 eV full width at half-maximum (for the Si 2p photopeak).[17] The binding energy scale of the XPS spectra was calibrated to the Si 2p feature of the bulk at 99.3 eV.[38] Spectral fitting and deconvolution based on residual minimization with Gaussian−Lorentzian line shapes were performed by using the CasaXPS software. For temperature-dependent XPS measurements, the sample was flash-annealed to the preselected temperature and quenched to RT before collecting the XPS spectra. The quantification of the Cl content on the surface based on the Cl 2p photopeak at 200 eV is often obscured by the ill-defined background contribution arising from the nearby Si 2s feature (at 151 eV). To avoid such ambiguity, the Cl 2s photopeak was used instead in all the experiments.

A 14×7 mm^2 substrate was cut from a single-sided polished p-type B-doped Si(100) wafer (0.4 mm thick) with a resistivity of 0.0080−0.0095 Ω cm. Details of the sample mounting and preparation procedures have been described in our earlier work.[15,17] The liquid chlorinated benzene chemicals, MCB (99.9% purity) and 1,3-DCB (98% purity), were purchased from Aldrich and thoroughly degassed by repeated freeze−pump−thaw cycles prior to use. The chemicals were exposed to the Si sample by backfilling the preparation chamber to an appropriate pressure (as monitored by an uncalibrated ionization gauge) with a variable precision leak valve. All exposures (in units of Langmuir, $1\ \text{L} = 1 \times 10^{-6}$ Torr•s) were performed at RT, and a saturation coverage was used unless stated otherwise.

All the calculations were performed by using methods based on the density functional theory (DFT) at the B3LYP level with the 6-31G(d) basis set in the Gaussian 03 package.[39] Frequency calculations were also performed for all the optimized structures in order to identify the local minima as equilibrium structures. A double-dimer section of the Si(100)2×1 surface was approximated by using the surface of a $Si_{15}H_{16}$ cluster. Both geometries of the cluster and the adsorbate were fully relaxed in all the calculations in order to obtain reliable frequency values. The adsorption energy corresponds to the energy difference between the total energy of an optimized adsorption structure and that of the $Si_{15}H_{16}$ cluster and a free chlorinated benzene molecule (with the zero-point vibrational energy corrections included in all the total energies). We also repeated our calculations using a larger basis set with more polarization and/or diffuse functions [e.g., 6-31+G(d)]. Although the larger basis sets generally led to lower total energies, the orderings of the total energies and relative stabilities of the adstructures were found to follow those obtained at the 6-31G(d) level. The use of the simpler basis set in the present calculations would therefore not affect the qualitative conclusions obtained in the present work. Although a multireference wave function has been recently suggested to provide a better simulation of the bare silicon surface,[25] the physical interpretation of this type of sophisticated wave functions is not trivial. It is therefore still of interest to use the DFT method, along with a single-configuration wave function of a relatively modest Gaussian basis set, to qualitatively identify the plausible adstructures.

3. Results and Discussion

3.1. RT Adsorption. Figure 1 compares the Cl 2s and C 1s XPS spectra of 50 L exposures of both MCB and 1,3-DCB to Si(100)2×1 at RT with that of 1,2-DCB. In accord with our previous assignment for 1,2-DCB (Figure 1c),[27] the C 1s feature at 284.6 eV (C_1) for both MCB (Figure 1a) and 1,3-DCB (Figure 1b) could be attributed to the C−H and/or C−Si bond, while the C 1s feature at 286.0 eV (C_2) could correspond to the C−Cl bond. This assignment is also in good accord with that used for benzene adsorption on Si(100)2×1,[27,40] for which a single C 1s feature corresponding to the C−H and/or C−Si bond is observed at 284.6 eV. It should be noted that the instrumental

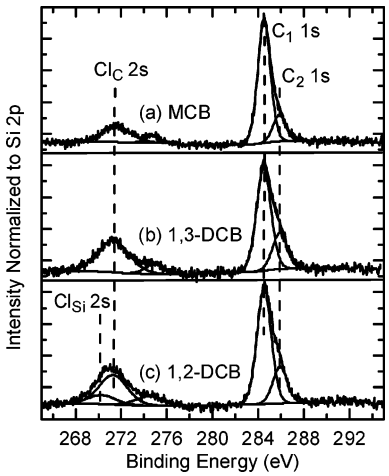

Figure 1. C 1s and Cl 2s XPS spectra of 50 L of (a) MCB, (b) 1,3-DCB, and (c) 1,2-DCB exposed to Si(100)2×1 at RT.

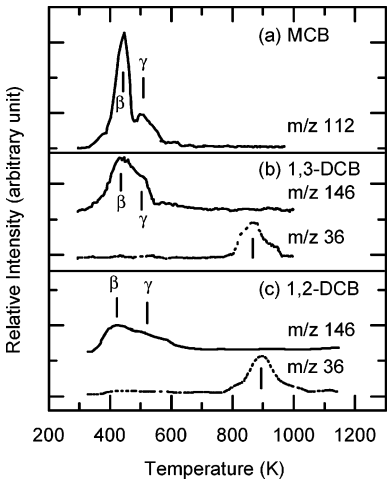

Figure 2. TPD profiles of *m*/*z* 112 ($C_6H_5Cl^+$) for (a) 50 L of MCB, and *m*/*z* 146 ($C_6H_4Cl_2^+$) and 36 (HCl^+) for 50 L of (b) 1,3-DCB and (c) 1,2-DCB exposed to Si(100)2×1 at RT.

energy resolution in the present XPS setup or indeed a synchrotron radiation XPS setup with a higher energy resolution[40] is not sufficient to resolve the C 1s chemical shifts of the C sp^3 (at ∼284.2 eV) and sp^2 (at ∼284.0 eV) hybridized bonding features.[40,41] Furthermore, neither setup can resolve the close-lying C 1s features for C−Si (at 283.9−284.3 eV) and C−H (at 284.0−284.6 eV),[40] which are due to similar electronegativities of Si (1.8, Pauling scale) and H (2.1).[42] The observed C_1 feature at 284.6 eV could therefore have contributions from the C−Si and/or C−H bonding and/or any other type of hydrocarbon adspecies with C sp^3 and sp^2 components on the surface. On the other hand, the C_2 1s feature at a higher binding energy (286.0 eV) could only be reasonably assigned to the C−Cl bonding, given the large electronegativity for Cl (3.16).[42] Given that the bond strength for C−H (81 kcal/mol) is larger than that of Si−H (72 kcal/mol), while that of C−Cl (95 kcal/mol) is smaller than that of Si−Cl (98 kcal/mol),[43] we consider that the dissociative adsorption of chlorinated benzenes could most likely involve the breakage of C−Cl bonds (i.e., dehalogenation) and not the breakage of C−H bonds (dehydrogenation). The ratio of the C_1 1s to C_2 1s intensities could therefore be used to indicate the degree of C−Cl dissociation, as discussed in our previous work.[27] For example, a C_1/C_2 intensity ratio of 3.0 found for 1,2-DCB suggests that 25% of the C−Cl bonds in the adstructures have undergone cleavage upon adsorption.[27] The corresponding C_1/C_2 intensity ratios for MCB (5.0) and 1,3-DCB (2.0), however, are found to be the same as the respective stoichiometric ratios of the C−H to C−Cl bonds in MCB and 1,3-DCB. This result indicates that both MCB and 1,3-DCB predominantly adsorb on Si(100)2×1 molecularly, without C−Cl dissociation. Furthermore, the total C 1s intensities relative to the respective Si 2p intensities for MCB (0.074), 1,3-DCB (0.069), 1,2-DCB (0.089), and benzene (0.078) are found to be reproducible. The adsorption of benzene has been shown to be molecular, with one adsorbate per two dimers, by Taguchi et al.[14] The smaller C 1s intensities found for MCB and 1,3-DCB with respect to that for benzene indicate their correspondingly smaller coverages compared to that of benzene. The smaller coverages suggest that there could be a stronger adsorbate−adsorbate interaction for MCB or 1,3-DCB compared to that for benzene, with the former (MCB) being less notable than the latter (1,3-DCB). On the other hand, the larger C 1s intensity found for 1,2-DCB with respect to that for benzene indicates a coverage larger than that of benzene, suggesting that the corresponding dissociation products could rearrange on the surface to provide a more efficient surface packing of the adstructures. These differences suggest that the chlorine content and the relative Cl substitutional locations on the benzene ring could affect the coverage of the adstructures on the 2×1 surface.

Given the nature of the adsorption inferred from the C 1s spectra, we have employed a single peak to fit the Cl 2s feature observed at 271.2 eV for MCB (Figure 1a) and 1,3-DCB (Figure 1b) and attributed it to the C−Cl bonding.[44] For 1,2-DCB (Figure 1c), two peaks were used to fit the Cl 2s envelop, and the two deconvoluted features at 270.3 eV (Cl_{Si}) and 271.2 eV (Cl_C) were assigned to Si−Cl and C−Cl bonding components, respectively, in our previous work.[27] The weak Cl 2s feature located at 274.2 eV for MCB and 1,3-DCB could be assigned as a shake-up peak, following our earlier assignment for 1,2-DCB.[27] It is of interest to note that the shake-up peaks for MCB and 1,3-DCB (and 1,2-DCB) are located at a higher binding energy (274.2 eV) than that observed for the corresponding shake-up features (273.9 eV) for chlorinated ethylenes on Si(100)2×1.[45] The Cl 2s shake-up features in chlorinated ethylenes and chlorinated benzenes are found to shift consistently with the corresponding main Cl 2s features and independently of the flash-annealing temperature, further supporting the assignment of these features to shake-up processes. The total Cl 2s intensities relative to that of the Si 2p peak at 99.3 eV are found to be 0.016, 0.027 and 0.035 for MCB, 1,3-DCB and 1,2-DCB,[27] respectively. The lower Cl 2s relative intensity for 1,3-DCB than that for 1,2-DCB is consistent with the lower coverage of 1,3-DCB inferred from the corresponding C 1s spectra. From partial dissociative adsorption for 1,2-DCB to exclusive molecular adsorption for 1,3-DCB, the adsorption behaviors of the two DCB isomers on Si(100)2×1 are therefore found to be notably different. Differences in the relative Cl positions on the benzene ring in the two isomers could therefore greatly affect the nature of the adstructures and their subsequent reaction pathways on the 2 × 1 surface.

3.2. Thermal Evolution Studies. Figure 2 compares the TPD profiles of selected mass fragments for MCB and 1,3-DCB with those of 1,2-DCB,[27] all exposed with a saturation coverage (50 L) to Si(100)2×1 at RT. Like benzene on Si(100)2 × 1,[10,14,27] MCB exhibits only desorption features for the parent ion $C_6H_5Cl^+$ (*m*/*z* 112): β state at 450 K and γ state at 510 K (Figure 2a). Other fragments, including $C_6H_6^+$ (*m*/*z* 68), HCl^+ (*m*/*z* 36), $C_2H_4^+$ (*m*/*z* 28), $C_2H_2^+$ (*m*/*z* 26), and H_2^+ (*m*/*z* 2), have also been monitored but no desorption features were found. For 1,3-DCB (Figure 2b), our TPD experiments also monitored a range of possible fragment ions, including the parent ion $C_6H_4Cl_2^+$

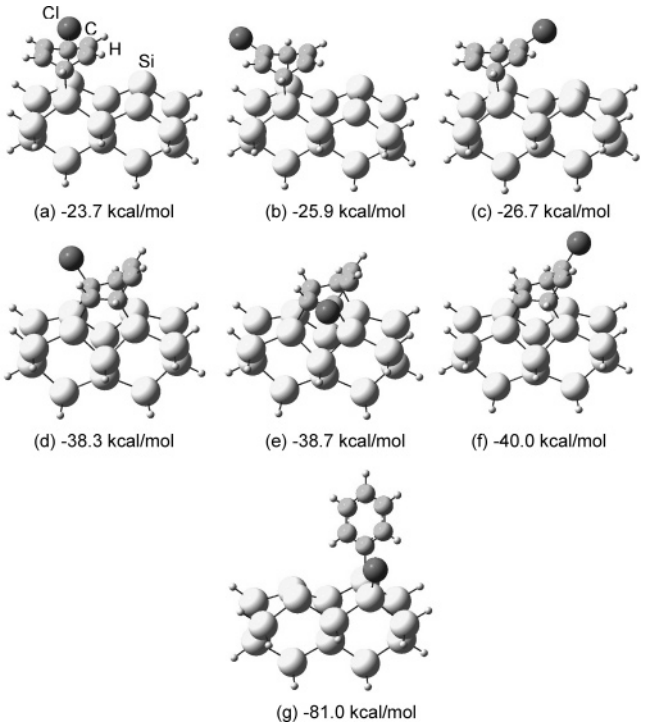

Figure 3. Equilibrium geometries of plausible adstructures for MCB on a model 2×1 surface of a $Si_{15}H_{16}$ cluster (with the Si dimer row oriented from left to right). The structures and their corresponding adsorption energies are obtained by density functional calculations at the B3LYP/6-31G(d) level. The molecular adstructures include three di-σ-bonded chloro-CHDD isomers (a−c) and three tetra-σ-bonded chloro-CHT isomers (d−f). The single-dechlorinated phenyl adstructure is shown in panel g.

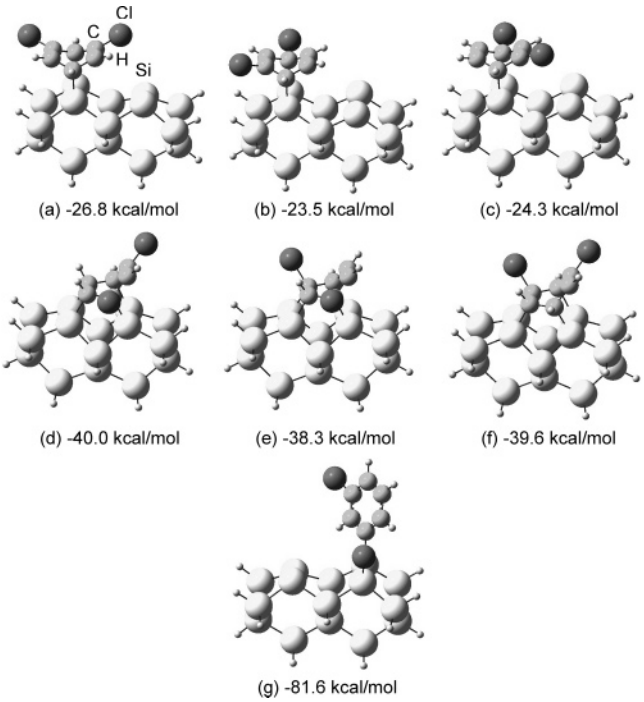

Figure 4. Equilibrium geometries of plausible adstructures for 1,3-DCB on a model 2×1 surface of a $Si_{15}H_{16}$ cluster (with the Si dimer row oriented from left to right). The structures and their corresponding adsorption energies are obtained by density functional calculations at the B3LYP/6-31G(d) level. The molecular adstructures include three di-σ-bonded dichloro-CHDD isomers (a−c) and three tetra-σ-bonded dichloro-CHT isomers (d−f). The single-dechlorinated chlorophenyl adstructure is shown in panel g.

(*m*/*z* 146), $C_6H_6^+$ (*m*/*z* 68), HCl^+ (*m*/*z* 36), $C_2H_4^+$ (*m*/*z* 28), $C_2H_2^+$ (*m*/*z* 26), and H_2^+ (*m*/*z* 2). Like the TPD profiles of 1,2-DCB,[27] only the profiles for *m*/*z* 146 (parent ion) and *m*/*z* 36 reveal any discernible features. Following the assignments made in our recent work,[27] the molecular desorption features at 450 K (β state) and near 510 K (γ state) for both 1,3-DCB (Figure 2b) and MCB (Figure 2a) could be attributed to the corresponding chlorinated derivatives of a cyclohexa-2,5-diene-1,4-diyl (CHDD) and a 5-cyclohexene-1,2,3,4-tetrayl (CHT) adstructure, respectively, found for the benzene adsorption. Similarly, the *m*/*z* 36 TPD feature observed at 880 K for 1,3-DCB (Figure 2b) could correspond to recombinative HCl desorption, in accord with our assignment for the *m*/*z* 36 feature found at 900 K for 1,2-DCB (Figure 2c).[27] The presence of HCl desorption for 1,3-DCB (and 1,2-DCB) on the 2×1 surface suggests that the C−Cl and C−H bond breakage could occur at an elevated temperature below 900 K. Any undissociated H could remain with the carbon fragments on the surface to form hydrocarbon clusters (as found in our temperature-dependent XPS data discussed in section 3.4 below).

3.3. Calculated Adstructures. To gain further insight into the nature of possible adstructures, we performed ab initio DFT calculations at the B3LYP/6-31G(d) level using the double-dimer surface of a $Si_{15}H_{16}$ cluster as the model for the Si(100)2×1 surface. The present calculations are not intended to be exhaustive, and only the more reasonable adsorption configurations have been included. Equilibrium geometries of both molecular and dechlorinated adstructures and their adsorption energies have been obtained for MCB and 1,3-DCB on Si(100)2×1 and are shown in Figures 3 and 4, respectively. These results are compared with those obtained for the other DCB isomers: 1,2-DCB, as reported previously in our recent work,[27] and 1,4-DCB, shown in Figure 5. Evidently, common molecular and dissociated adstructures could be identified for MCB and the DCB isomers. In particular, three molecular isomer adstructures, each involving the chlorinated derivatives of CHDD (Figures 3 and 4, panels a−c) and CHT (Figures 3 and 4, panels d−f), have been obtained for MCB (Figure 3) and 1,3-DCB (Figure 4). Two dichloro-CHDD isomer adstructures have been determined for both 1,2-DCB[27] and 1,4-DCB (Figure 5a,b), while four and two dichloro-CHT isomer adstructures are obtained for 1,2-DCB[27] and 1,4-DCB (Figure 5c,d), respectively. Furthermore, the adsorption energies for all of the chlorinated CHDD adstructures are similar and are generally less negative by at least 11.5 kcal/mol than those of the corresponding chlorinated CHT adstructures (the adsorption energies of which are also similar to one another). The less stable di-σ-bonded chlorinated CHDD adstructures could therefore be attributed to the lower-temperature state (β state) in the molecular desorption profiles of MCB (Figure 2a) and 1,3-DCB (Figure 2b). Similarly, the more stable tetra-σ-bonded chlorinated CHT adstructures could be responsible for the corresponding higher-temperature desorption states (γ state). In addition, although the differences in the adsorption energies among the isomer adstructures are very small, the isomer adstructures containing more ipso-C atoms attached to a Cl atom (Figures 3a, 4b,c, and 5a for CHDD and Figures 3d,e, 4d−f, and 5c,d for CHT) are generally less stable (i.e., with less negative adsorption energies) than the corresponding isomer adstructures without these types of Cl-decorated ipso-C atoms (Figures 3b,c, 4a, and 5b for CHDD and Figure 3f for CHT). For example, the adsorption energies for the chloro-CHDD adstructure shown in Figure 3a are less negative than that for the chloro-CHDD adstructures shown in Figure 3b,c. This trend suggests that the initial adsorption would favor the C position

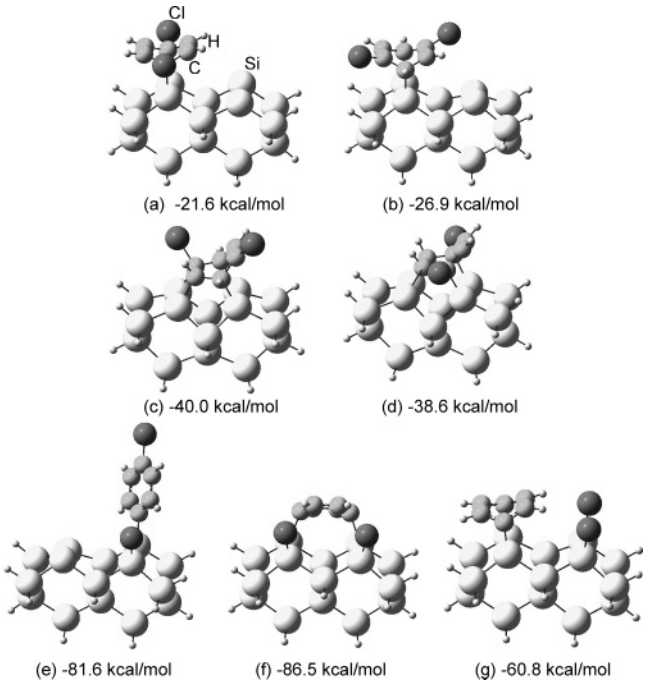

Figure 5. Equilibrium geometries of plausible adstructures for 1,4-DCB on a model 2×1 surface of a $Si_{15}H_{16}$ cluster (with the Si dimer row oriented from left to right). The structures and their corresponding adsorption energies are obtained by density functional calculations at the B3LYP/6-31G(d) level. The molecular adstructures include two di-σ-bonded dichloro-CHDD isomers (a,b) and two tetra-σ-bonded dichloro-CHT isomers (c,d). The dissociated adstructures include one single-dechlorinated chlorophenyl adstructure (e) and two double-dechlorinated 1,4-phenylenes in the cross-dimer (f) and in-dimer (g) sites.

without the Cl atom attached, which appears to be reasonable considering the steric hindrance effects exerted by the Cl atoms.

In the case of dissociative adsorption, the adsorption energies for the dechlorinated adstructures are more negative than those for the corresponding molecular adstructures for MCB (Figure 3g) and 1,3-DCB (Figure 4g). On the other hand, the lack of any dechlorinated product observed for MCB on Si(100)2×1 suggests that kinetics plays a more prominent role than thermodynamics in controlling the adsorption pathways. In the case of 1,4-DCB, one single-dechlorinated chlorophenyl (Figure 5e) and two double-dechlorinated 1,4-phenylenes (Figure 5f,g) have been obtained in our calculation. In the case of single dechlorination, the adsorption energy of the chlorophenyl adstructure for 1,4-DCB (−81.6 kcal/mol, Figure 5e) is essentially identical to those for 1,3-DCB (−81.6 kcal/mol, Figure 4g) and 1,2-DCB (−83.0 kcal/mol).[27] In contrast, the adsorption energies of the double-dechlorinated in-dimer 1,4-phenylene (−60.8 kcal/mol, Figure 5g) and the cross-dimer 1,4-phenylene (−86.5 kcal/mol, Figure 5f) for 1,4-DCB are considerably less negative than those of the respective in-dimer 1,2-phenylene (−135.8 kcal/mol) and cross-dimer 1,2-phenylene (−146.0 kcal/mol) for 1,2-DCB.[27] The 1,4-phenylene adstructures with the buckled benzene ring parallel to the Si surface (Figure 5f,g) are evidently less stable than the corresponding 1,2-phenylene adstructures with the planar benzene ring perpendicular to the Si surface.[27] Distortion to the planar ring structure could be responsible for the reduced stability of the 1,4-phenylene (Figure 5f,g) in comparison to the 1,2-phenylene adstructure.[27]

Our calculations also show that the attachment of an electron-withdrawing ligand such as the Cl atom to the benzene ring would affect the energy levels of the highest occupied molecular orbital (HOMO) and the lowest unoccupied molecular orbital (LUMO) (relative to those of benzene), thereby changing the HOMO−LUMO energy gap. This energy gap decreases with more Cl substitution on the benzene ring. We have estimated that the energy gaps of the free molecules at the B3LYP/6-31G(d) level are 6.8 eV for benzene, 6.4 eV for MCB, 6.2 eV for 1,3-DCB and 1,2-DCB, and 6.0 eV for 1,4-DCB. By polarizing the benzene ring, the electron-withdrawing Cl atoms also enhance the [2+4] cycloaddition reaction on Si(100)2×1.[46] However, the adsorbate−adsorbate interaction on the surface or the steric hindrance effect as a result of the Cl substitution on the benzene ring may cancel this enhancement. This cancellation could explain the similar molecular desorption temperatures found for chlorinated benzenes compared to those of benzene on the 2×1 surface in our TPD experiments.[27] In the case of adsorbed halogenated benzenes, the calculated energy gaps of all the halogenated benzene on the $Si_{15}H_{16}$ cluster for CHDD adstructures are very similar to that of benzene, which is approximately 2.3 eV. This calculation result indicates that Cl substitution does not perturb the electronic structures of the adsorption species upon molecular adsorption of chlorinated benzene on Si(100)2×1. Upon double Cl abstraction to the silicon surface in the case of 1,2-DCB on the $Si_{15}H_{16}$ cluster, a noticeable increase in the energy gap to 4.5 eV has been observed for the resulting phenylene adspecies. The presence of partial dissociation only in the case of 1,2-DCB could be due to the structural compatibility between the Cl-to-Cl separation (3.22 Å) of the incoming admolecule and the in-dimer Si-to-Si spacing (2.25 Å). The [2+4] cycloaddition reaction of benzene on Si(100)2×1 has been found to be a concerted reaction (i.e., without any precursor states), in which a six π-electron transition state is formed, similar to the classical case of the [2+4] reaction discussed in solution-phase organic chemistry.[46] It is therefore reasonable to expect that similar transition states could also occur for the adsorption of chlorinated benzenes on the 2 × 1 surface. In Scheme 1a, we propose a possible configuration of this transition state for the adsorption of 1,2-DCB on Si(100)2×1. Because Cl substitution at the C1 and C2 positions of the benzene ring causes the steric hindrance on C1 and C2, the dangling bonds at the Si dimer atoms (in the cross-dimer configuration) could readily attack the C3 and C6 atoms. The subsequent interactions between the neighboring Si dimer atoms and the two Cl atoms on the same side of the anchor points (C3 and C6) in 1,2-DCB could initiate the C−Cl dissociation (at the C1 and C2 positions). On the other hand, Cl substitution at the C1 and C3 positions as in 1,3-DCB (Scheme 1b) or at the C1 and C4 positions as in 1,4-DCB (Scheme 1c) would lead to cycloaddition at the C2 and C5 positions. The distribution of the Cl atoms on either side of the anchor points (C2 and C5) does not facilitate C−Cl dissociation.

SCHEME 1. Schematic Diagram of Possible Molecular Arrangements Leading to (a) Double-Dechlorination of 1,2-DCB, and (b) Cycloaddition of 1,3-DCB and (c) 1,4-DCB[a]

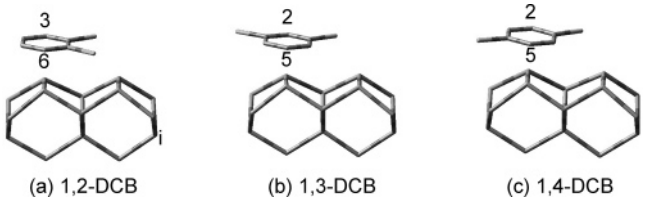

[a] The initial attack sites for 1,2-DCB favor C3 and C6, while those for 1,3-DCB and 1,4-DCB favor C2 and C5. It should be noted that only one DCB molecule (with the two C−Cl bonds represented) interacting with two surface dimers (four surface Si atoms) is shown.

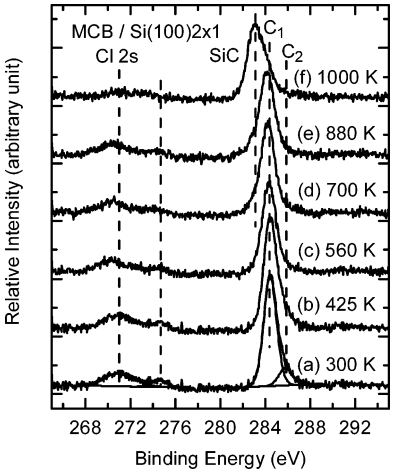

Figure 6. XPS spectra of the C 1s and Cl 2s regions of 50 L of MCB exposed to Si(100)2×1 at (a) 300 K, and upon sequential flash-annealing to (b) 425 K, (c) 560 K, (d) 700 K, (e) 880 K, and (f) 1000 K.

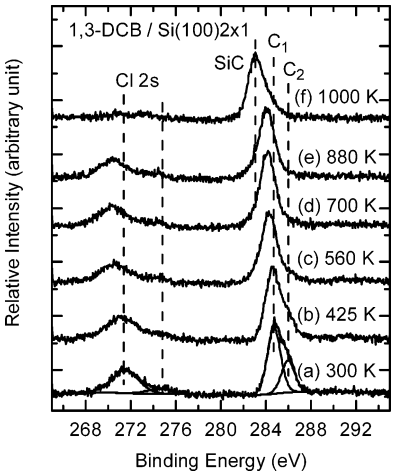

Figure 7. XPS spectra of the C 1s and Cl 2s regions of 50 L of 1,3-DCB exposed to Si(100)2×1 at (a) 300 K, and upon sequential flash-annealing to (b) 425 K, (c) 560 K, (d) 700 K, (e) 880 K, and (f) 1000 K.

This situation is similar to that for MCB, for which no dissociative adsorption is observed. The exact mechanisms and kinetic factors that control these two pathways (dissociation vs cycloaddition) remain unclear and will be further investigated in future work.

3.4. Temperature-Dependent XPS Studies. The thermal evolution of the adstructures can be further elucidated by following the changes in the XPS spectra upon sequentially flash-annealing the sample to different temperatures. Figures 6 and 7 show the Cl 2s and C 1s XPS spectra as a function of the flash-annealing temperature for 50 L of MCB and 1,3-DCB exposed to Si(100)2×1 at RT, respectively. The corresponding temperature profiles of the respective intensities of the C_1 1s, C_2 1s, C_{total} 1s, Cl_{Si} 2s (Cl bonding to Si), and Cl_C 2s (Cl bonding to C) features relative to the intensity of the Si 2p feature at 99.3 eV are summarized in Figure 8. Evidently, the spectral changes of the thermal processes for MCB (Figure 6) and 1,3-DCB (Figure 7) are found to be similar to each other. In particular, upon annealing the sample to 425 K, a slight increase in the intensity for the C_1 1s feature at 284.6 eV is observed, along with a concomitant decrease for the C_2 1s feature at 286.0 eV. The corresponding peak locations of these C 1s features remain essentially unchanged for MCB (Figure 6b) and 1,3-DCB (Figure 7b). This result indicates that Cl abstraction occurs

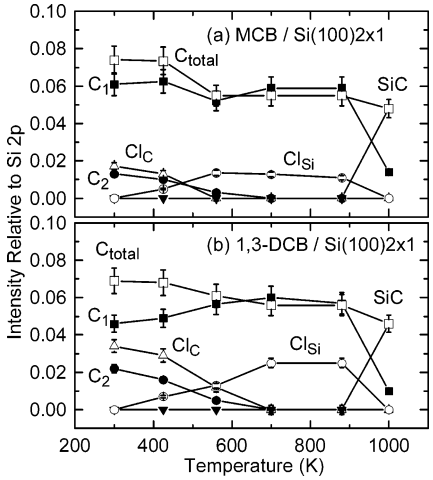

Figure 8. Spectral intensities of various C 1s and Cl 2s features for 50 L of (a) MCB and (b) 1,3-DCB exposed to Si(100)2×1 at RT and as a function of the flashing-annealing temperature, all relative to the spectral intensity of the Si 2p feature at 99.3 eV. The C 1s features include C_1 1s at 284.6 eV (■), C_2 1s at 286.0 eV (●), SiC at 283.0 eV (▼), and C_{total} 1s (□, corresponding to the sum of all three C 1s components), while the Cl 2s features include Cl_C at 271.2 eV (△) and Cl_{Si} at 270.3 eV (○), corresponding to the respective Cl 2s features of the Cl−C and Cl−Si bonds.

at a rather low temperature of 425 K, which in turn suggests a relatively low activation barrier for the dissociation of the C−Cl bond. Flash-annealing the sample to 560 K (Figures 6c and 7c) reduces both the Cl 2s and total C 1s intensities, in good accord with our TPD results that show molecular desorption near 450−510 K for MCB (Figure 2b) and 1,3-DCB (Figure 2c). Further decrease in the C_2 1s intensity with a corresponding increase in the C_1/C_2 intensity ratio is also observed, which suggests further Cl abstraction. The completion of Cl abstraction at 700 K is marked by the total disappearance of the C_2 1s intensity (Figures 6d, and 7d) and a notable increase in the C_1 1s intensity, while the total intensity for the Cl 2s features remains unchanged from 560 to 700 K. Further flash-annealing the samples to 880 K (Figures 6e and 7e) has no apparent effect on the C 1s and Cl 2s spectra. The migration of the C 1s peak maximum to 1000 K from 700 K for MCB and from 560 K for 1,3-DCB is due to the onset of hydrocarbon decomposition processes and the emergence of a new C 1s feature corresponding to SiC at 283.0 eV. The small but discernible shoulder near the C_1 1s location is consistent with the presence of clusters of carbon and/or hydrocarbon (generally with a C 1s binding energy of 284.0−284.8 eV).[45] At the annealing temperature of 1000 K (Figures 6f and 7f), the Cl 2s feature totally disappears while the SiC feature at 283.0 eV becomes the most prominent feature. The removal of Cl is consistent with the recombinative HCl desorption observed near 900 K in our TPD experiment for 1,3-DCB (Figure 2b). However, the absence of HCl desorption and any Cl-related species above the 560 K found in the corresponding TPD data for MCB could not explain the observed Cl 2s spectral evolution above 560 K (Figure 6d−f). The presence of minor Cl-containing adspecies above 560 K may suggest possible readsorption of desorbed species back onto the still-hot surface during the cool-down of the sample to RT before acquiring the XPS spectrum. The apparent small fraction of molecular desorption, as indicated by the small reduction observed in the total C 1s intensities (Figure 8) at 560 K for MCB (26%) and 1,3-DCB (19%), is also consistent with the readsorption model.

4. Summary

The RT adsorption and thermal evolution of MCB and 1,3-DCB on Si(100)2×1 have been investigated by XPS and TPD and compared with that of 1,2-DCB.[27] Combined with the results from our DFT calculations, these experimental data are used to infer the effects of chlorine content and different DCB isomers on the plausible adstructures and adsorption mechanisms. The similarities obtained from the XPS and TPD results suggest that the adsorption primarily involves bonding through the benzene ring for all three chlorinated molecules (MCB, 1,3-DCB, and 1,2-DCB) on Si(100)2×1. In particular, the C_1/C_2 peak intensity ratios of 5.0 and 2.0 for MCB and 1,3-DCB, respectively, indicate that, like benzene, MCB and 1,3-DCB adsorb molecularly on the 2×1 surface at RT without any evidence for dissociation, in contrast to the partial dissociation found for 1,2-DCB.[27] All three chlorinated benzenes, MCB, 1,3-DCB, and 1,2-DCB, also exhibit similar molecular desorption states near 450 and 510 K, which could be assigned to di-σ-bonded chlorinated CHDD and tetra-σ-bonded chlorinated CHT adstructures, respectively. The partial dechlorination found only for 1,2-DCB and not MCB and 1,3-DCB suggests that kinetic effects could play an important role in determining the reaction pathways. Furthermore, dechlorination in 1,2-DCB could be due to a steric hindrance effect in the transition state, in which the locations of Cl atoms on the same side of the anchor points promote C−Cl bond dissociation.

Acknowledgment. This work was supported by the Natural Sciences and Engineering Research Council of Canada.

References and Notes

(1) James, D. K.; Tour, J. M. *Chem. Mater.* **2004**, *16*, 4423.
(2) Wilson, E. G. *Jpn. J. Appl. Phys.* **1995**, *34*, 3775.
(3) Roth, K. M.; Yasseri, A. A.; Liu, Z.; Dabke, R. B.; Malinovskii, V.; Schweikart, K.-H.; Yu, L.; Tiznado, H.; Zaera, F.; Lindsey, J. S.; Kuhr, W. G.; Bocian, D. F. *J. Am. Chem. Soc.* **2003**, *125*, 505.
(4) Hersam, M. C.; Guisinger, N. P.; Lyding, J. W. *Nanotechnology* **2000**, *11*, 70.
(5) Richter, C. A.; Hacker, C. A.; Richter, L. J.; Vogel, E. M. *Solid-State Electron.* **2004**, *48*, 1747.
(6) Gokhale, S.; Trischberger, P.; Menzel, D.; Widdra, W.; Dröge, H.; Steinrück, H.-P.; Birkenheuer, U.; Gutdeutsch, U.; Rösch, N. *J. Chem. Phys.* **1998**, *108*, 5554.
(7) Costanzo, F.; Sbraccia, C.; Silvestrelli, P. L.; Ancilotto, F. *Surf. Sci.* **2004**, *566*, 971.
(8) Borovsky, B.; Krueger, M.; Ganz, E. *J. Vac. Sci. Technol., B* **1998**, *17*, 7.
(9) Wang, G. T.; Mui, C.; Tannaci, J. F.; Filler, M. A.; Musgrave, C. B.; Bent, S. F. *J. Phys. Chem. B* **2003**, *107*, 4982.
(10) Li, Q.; Leung, K. T. *Surf. Sci.* **2003**, *541*, 113.
(11) Schwartz, M. P.; Ellison, M. D.; Coulter, S. K.; Hovis, J. S.; Hamers, R. J. *J. Am. Chem. Soc.* **2000**, *122*, 8529.
(12) Witkowski, N.; Hennies, F.; Pietzsch, A.; Mattsson, S.; Föhlisch, A.; Wurth, W.; Nagasono, M.; Piancastelli, M. N. *Phys. Rev. B* **2003**, *68*, 115408.
(13) Hamaguchi, K.; Mukai, K.; Yamashita, Y.; Yoshinobu, J.; Sato, T.; Iwatsuki, M. *Surf. Sci.* **2003**, *531*, 199.
(14) Taguchi, Y.; Fujisawa, M.; Nishijima, M. *Chem. Phys. Lett.* **1990**, *178*, 363.
(15) Li, Q.; He, Z. H.; Zhou, X. J.; Yang, X.; Leung, K. T. *Surf. Sci.* **2004**, *560*, 191.
(16) He, Z. H.; Yang, X.; Zhou, X. J.; Leung, K. T. *Surf. Sci. Lett.* **2003**, *547*, L840.
(17) Zhou, X. J.; Li, Q.; He, Z. H.; Yang, X.; Leung, K. T. *Surf. Sci.* **2003**, *543*, L668.
(18) He, Z. H.; Leung, K. T. *Surf. Sci.* **2003**, *523*, 48.
(19) Li, Q.; Leung, K. T. *Surf. Sci.* **2001**, *479*, 69.
(20) He, Z. H.; Leung, K. T. *Appl. Surf. Sci.* **2001**, *174*, 225.
(21) Flaum, H. C.; Sullivan, D. J. D.; Kummel, A. C. *J. Phys. Chem.* **1994**, *98*, 1719.
(22) Hamers, R. J. *Nature* **2001**, *412*, 489.
(23) Guisinger, N. P.; Basu, R.; Baluch, A. S.; Hersam, M. C. *Ann. N.Y. Acad. Sci.* **2003**, *1006*, 227.
(24) Lopinski, G. P.; Moffatt, D. J.; Wolkow, R. A. *Chem. Phys. Lett.* **1992**, *282*, 305.
(25) Jung, Y.; Gordon, M. S. *J. Am. Chem. Soc.* **2005**, *127*, 3131.
(26) Alavi, S.; Rousseau, R.; Seideman, T. *J. Chem. Phys.* **2000**, *113*, 4412.
(27) Zhou, X. J.; Leung, K. T. *Surf. Sci.*, submitted for publication, 2006.
(28) Sloan, P. A.; Hedouin, M. F. G.; Palmer, R. E.; Persson, M. *Phys. Rev. Lett.* **2003**, *91*, 118301.
(29) Lu, P. H.; Polanyi, J. C.; Rogers, D. *J. Chem. Phys.* **1999**, *111*, 9905.
(30) Harikumar, K. R.; Petsalakis, I. D.; Polanyi, J. C.; Theodorakopoulos, G. *Surf. Sci.* **2004**, *572*, 162.
(31) Chen, X. H.; Kong, Q.; Polanyi, J. C.; Rogers, D.; So, S. *Surf. Sci.* **1995**, *340*, 224.
(32) Lu, P. H.; Polanyi, J. C.; Rogers, D. *J. Chem. Phys.* **2000**, *112*, 11005.
(33) Naumkin, F. Y.; Polanyi, J. C.; Rogers, D.; Hofer, W.; Fisher, A. *Surf. Sci.* **2003**, *547*, 324.
(34) Naumkin, F. Y.; Polanyi, J. C.; Rogers, D. *Surf. Sci.* **2003**, *547*, 335.
(35) Coulter, S. K.; Hovis, J. S.; Ellison, M. D.; Hamers, R. J. *J. Vac. Sci. Technol., A* **2000**, *18*, 1965.
(36) Birkenheuer, U.; Gutdeutsch, U.; Rosch, N. *Surf. Sci* **1998**, *409*, 213.
(37) Li, Q.; Leung, K. T. *J. Phys. Chem. B* **2005**, *109*, 1420.
(38) Moulder, J. F.; Stickle, W. F.; Sobol, P. E.; Bomben, K. D., *Handbook of X-ray Photoelectron Spectroscopy*; Perkin-Elmer Corporation: Eden Prairie, MN, 1992.
(39) Frisch, M. J.; Trucks, G. W.; Schlegel, H. B.; Scuseria, G. E.; Robb, M. A.; Cheeseman, J. R.; Montgomery, J. A.; Vreven, T.; Kudin, K. N.; Burant, J. C.; Millam, J. M.; Iyengar, S. S.; Tomasi, J.; Barone, V.; Mennucci, B.; Cossi, M.; Scalmani, G.; Rega, N.; Petersson, G. A.; Nakatsuji, H.; Hada, M.; Ehara, M.; Toyota, K.; Fukuda, R.; Hasegawa, J.; Ishida, M.; Nakajima, T.; Honda, Y.; Kitao, O.; Nakai, H.; Klene, M.; Li, X.; Knox, J. E.; Hratchian, H. P.; Cross, J. B.; Adamo, C.; Jaramillo, J.; Gomperts, R.; Stratmann, R. E.; Yazyev, O.; Austin, A. J.; Cammi, R.; Pomelli, C.; Ochterski, J. W.; Ayala, P. Y.; Morokuma, K.; Voth, G. A.; Salvador, P.; Dannenberg, J. J.; Zakrzewski, V. G.; Dapprich, S.; Daniels, A. D.; Strain, M. C.; Farkas, O.; Malick, D. K.; Rabuck, A. D.; Raghavachari, K.; Foresman, J. B.; Ortiz, J. V.; Cui, Q.; Baboul, A. G.; Clifford, S.; Cioslowski, J.; Stefanov, B. B.; Liu, G.; Liashenko, A.; Piskorz, P.; Komaromi, I.; Martin, R. L.; Fox, D. J.; Keith, T.; Al-Laham, M. A.; Gonzalez, C. Y.; Pople, J. A. *Gaussian 03*, Gaussian, Inc.: Pittsburgh, PA, 2003.
(40) Fink, A.; Widdra, W.; Wurth, W.; Keller, C.; Stichler, M.; Achleitner, A.; Comelli, G.; Lizzit, S.; Baraldi, A.; Menzel, D. *Phys. Rev. B* **2001**, *64*, 045308-1.
(41) Siegbahn, K.; Nordling, C.; Johansson, G.; Hedman, J.; Hedén, P. F.; Hamrin, K.; Gelius, U.; Bergmark, T.; Werme, L. O.; Manne, R.; Bear, Y. *ESCA Applied to Free Molecules*; North-Holland: New York, 1969.
(42) Pauling, L. *The Nature of Chemical Bond*; Cornell University Press: Ithaca, NY, 1960.
(43) Weast, R. C., Ed. *CRC Handbook of Chemistry and Physics*, 64th ed.; CRC Press: Baton Raton, FL, 1983.
(44) Clark, D. T.; Kilcast, D.; Adams, D. B.; Musgrave, W. K. R. *J. Electron. Spectrosc. Relat. Phenom.* **1975**, *6*, 117.
(45) Zhou, X. J.; Leung, K. T. *Surf. Sci.* **2006**, *600*, 468.
(46) Bruice, P. Y. *Organic Chemistry*; Prentice-Hall: Upper Saddle River, NJ, 1998; p 316.